N63 21830

COMPARISON OF FLIGHT MEASURED HELICOPTER

ROTOR BLADE CHORDWISE PRESSURE DISTRIBUTIONS

AND TWO-DIMENSIONAL AIRFOIL CHARACTERISTICS

By James Scheiman and Henry L. Kelley
NASA Langley Research Center

For Presentation at the CAL-TRECOM Symposium on

Dynamic Loads Problems Associated With Helicopters

and V/STOL Aircraft, Buffalo, New York,

June 26-27, 1963

COMPARISON OF FLIGHT MEASURED HELICOPTER ROTOR BLADE CHORDWISE PRESSURE DISTRIBUTIONS AND TWO-DIMENSIONAL AIRFOIL CHARACTERISTICS

By James Scheiman and Henry L. Kelley
NASA Langley Research Center

SUMMARY

21830

A comparison is made between airfoil chordwise pressure distributions from helicopter rotor flight tests and static two-dimensional wind-tunnel tests. Differences in actual and two-dimensional-airfoil pressure distributions are shown to exist. These differences in airfoil characteristics are expected to amplify the blade flapwise and torsional vibratory forces determined from two-dimensional-airfoil data. Possible reasons for these airfoil differences are briefly discussed. The point is made that in endeavoring to confirm current refined theories of calculating section angle of attack, it is essential, in making data comparisons, that care be used to prevent these differences between actual and static two-dimensional-section data from obscuring the effectiveness of the angle-of-attack calculations.

INTRODUCTION

Experience has shown that the ability to perform an adequate structural dynamic analysis of the rotor blade is marginal. This lack of ability has generally been viewed as attributable to unknown air loads and in particular to unknown inflow velocities rather than to the applicability of two-dimensional-airfoil characteristics. This view has tended to be confirmed, for example, by the results of rotor test inflow velocity measurements and by the adequacy of predicting helicopter performance by use of two-dimensional airfoil data. In any case, both inflow velocities and actual airfoil characteristics must be known in order to perform a reasonably accurate dynamic blade analysis.

In regard to the inflow velocities, it is believed that the capability of theory to predict these velocities for trim level flight has significantly improved recently. With these new theories the danger exists for blaming the remaining inadequacy of the inflow theory for any lack of correlation between test and theory, when the differences may actually be caused by airfoil characteristic discrepancies.

The validity of two-dimensional data has been given little detailed attention because of a lack of actual operating test data. Partly to help fill this gap, the NASA Langley Research Center has recently completed a helicopter flight-test program which has utilized extensive blade pressure instrumentation. These data provide a comparison of the actual and two-dimensional-airfoil chordwise pressure distributions to the extent needed to illustrate that important airfoil characteristic discrepancies do occur in the flight conditions sampled.

Portions of the flight measured chordwise pressure distributions for two flight conditions are discussed. Samples of these distributions are directly compared with two-dimensional full-scale data (see ref. 1) by equating the two normal force coefficients. The chordwise pressure distribution for other flight conditions and the movement of the blade center of pressure are discussed.

All reference to two-dimensional-airfoil characteristics in this paper refers to static two-dimensional characteristics in distinction to oscillating unsteady two-dimensional characteristics.

SYMBOLS

c	airfoil chord
C_N	normal-force coefficient
Δp	differential pressure measured on the airfoil
q	dynamic pressure
r	radial distance to blade element measured from center of rotation
R	blade radius measured from center of rotation
V_F	forward speed
x	chordwise distance measured from blade leading edge
$\bar{x}$	center of pressure of airfoil section measured from leading edge
μ	nondimensional tip-speed ratio, $\frac{1.69V_F}{\Omega R}$
ψ	blade nominal azimuth angle, measured from downwind position in the direction of rotation and disregarding blade lag motion
Ω	rotor angular velocity

DISCUSSION

Normal-Force Coefficient for Flight With Blade Section Stall

A plot of the local normal-force coefficients C_N along the blade radius for different azimuth positions is shown in figure 1. The flight condition is for a trim, level-flight-cruise forward speed and a reduced rotor rotational speed and is thus for a flight condition expected to produce local blade-section stalling. Further details of this flight condition are available in table IV of reference 2.

Notice the high values of normal-force coefficient in the area of $r/R = 0.55$, $\psi = 210^\circ$ to $\psi = 240^\circ$ and for $r/R = 0.75$, $\psi = 250^\circ$. These coefficients correspond to dynamic pressures of approximately 50 pounds per square foot at $r/R = 0.55$ and 100 pounds per square foot at $r/R = 0.75$. The normal-force coefficient values, in these areas of the rotor, correspond to values above the maximum static two-dimensional values of C_N. Just prior to these high normal-force coefficients a rapid rate of change in the normal-force coefficient is noted. This change in C_N can be directly related to a two-dimensional-airfoil angle-of-attack change and the corresponding high rates of angle-of-attack change can be explained, for example, by the rapid changes in local inflow velocities through the rotor. In this instance an estimate based on successive normal-force coefficients, in the previously mentioned high angle-of-attack area of the rotor, indicates a rate of roughly 100° per second or 1° per 2-1/2 blade-chord lengths. This rapid angle-of-attack increase will provide a partial explanation for the lack of chordwise-pressure-distribution correlation explored further in this paper.

The circles on this figure are points where chordwise pressure distributions are discussed in figures 2 to 4; the solid circles are points where two-dimensional and flight data are compared.

Chordwise Pressure Distributions for Flight With Blade Section Stall

Figures 2 to 4 are for the same flight condition as figure 1, which was selected with the expectation of producing local blade-section stalling. A plot of the chordwise pressure coefficient distribution for $r/R = 0.55$ and $\psi = 165^\circ$, 195°, 210°, 225°, and 255° is shown in figure 2. The blade-azimuth position, integrated normal-force coefficient, and the centers of pressure are as indicated. At $\psi = 165^\circ$, the flight-test distribution agrees with the two-dimensional data; the center of pressure is close to (slightly aft of) the quarter chord. The normal-force coefficient is below the two-dimensional stall point. At $\psi = 195^\circ$ the normal-force coefficient of 1.3 is above the two-dimensional stall value but the pressure distribution appears unstalled. At the remaining azimuth locations the normal-force coefficient is above the airfoil section two-dimensional stall point and no two-dimensional data are available for comparison. The pressure distribution is such as to correspond to some separation and, therefore, the section can be viewed as exhibiting stall characteristics although the details of the distribution have no counterpart in two-dimensional data. Based on examination of the contours of figure 1, this increased maximum C_N

is expected to increase the vibratory amplitude of the actual airfoil blade loads as compared with the predicted two-dimensional air loads.

It may be of interest that some variations in pressure occurred between rotor revolutions for these last three plots (average values are shown); however, the distribution shapes are believed representative. These variations in themselves suggest a stalled type of flow.

Sample pressure distributions for $r/R = 0.75$ are shown in figure 3; these distributions are for the same flight condition shown in figures 1 and 2. For $\psi = 165^{\circ}$ and 195° the distribution shows good agreement with two-dimensional data. As the azimuth angle increases from $\psi = 195^{\circ}$ to 240°, the normal-force coefficients again increase to values above the two-dimensional stall point, although the actual airfoil retains the unstalled two-dimensional pressure distribution.

The pressure distribution for $r/R = 0.95$ is shown in figure 4. The normal-force coefficients are all below the static two-dimensional stall point and therefore good pressure-distribution correlation would be expected. For $\psi = 45^{\circ}$ and 75° the agreement between the flight and two-dimensional data is indeed reasonable, but at $\psi = 90^{\circ}$ and 120° the correlation is not so good. Thus, while a large part of the rotor does behave in accordance with two-dimensional data, figures 2 to 4 show that poor correlation can occur to a degree which would be expected to have a major effect on periodic blade loads.

Chordwise Pressure Distributions for Flight

With High Blade-Tip Mach Numbers

The next trim level flight condition discussed for flight at a high tip Mach number, for which the maximum blade-tip Mach number was 0.76. The chordwise pressure distribution for the 0.95 blade station is shown in figure 5. The normal-force coefficients are all below the two-dimensional-airfoil stall point and good correlation would be expected. The centers of pressure, however, are all farther forward than would be expected, even for high Mach number operation of a two-dimensional airfoil. For $\psi = 30^{\circ}$ there is reasonable agreement between the flight and two-dimensional distributions, although for $\psi = 75^{\circ}$, 90°, and 105° the flight data depart from the two-dimensional data.

The 0.75-radius station shown in figure 6 is for the previously described high tip Mach number flight. The flight-measured chordwise pressure distributions, the centers of pressure, and normal-force coefficients are typical of unstalled two-dimensional data. The correlation shown is good.

The high tip Mach number test for the 0.55-blade-span station is shown in figure 7. Again the normal-force coefficients, centers of pressure, and the distribution are typical of two-dimensional data. The correlation with two-dimensional data is again good.

In summary, figures 5, 6, and 7 for the high tip Mach number flight indicate that a large percentage of the actual chordwise pressure distributions are in agreement with two-dimensional airfoil data. Only a small (though important) percentage of the pressure distributions are not in agreement. Since the disagreement in this case is primarily in the high Mach number regions, it appears that with careful selection of the flight test conditions, it will be possible to find cases that warrant comparison with theories using the two-dimensional data to study the adequacy of new angle-of-attack prediction theories.

Other Flight Conditions

A small portion of the chordwise pressure distributions for a number of other trim level-flight conditions have been reviewed and the results were similar to the results of the previous two flight conditions discussed in detail in this paper; namely, that portions of the actual operating helicopter blade do not behave in accordance with two-dimensional airfoil data. Because there are these cases where important differences do arise, an exact knowledge of the rotor inflow velocities is not necessarily sufficient to describe the exact rotor blade loading. Caution should therefore be exercised in interpreting the correlation of flight measured and theoretical rotor-blade spanwise loadings.

Measured Center-of-Pressure Movement

In an attempt to generalize the actual airfoil center-of-pressure movement, a plot was made of the center of pressure as a function of the blade azimuth angle for three different flight conditions, and this plot is shown in figure 8. Note the forward shift in center of pressure on the advancing side of the rotor for all three flight conditions and the rearward center of pressure on the retreating side of the rotor for the first flight condition (flight with blade section stall discussed previously). The forward shift in center of pressure could not be explained by Mach number effects.

The flight-test blade was a modified NACA 0012 airfoil (ref. 1) and hence had no camber. The interesting possibility thus arises that if a small amount of camber, which would tend to add a constant moment coefficient with varying angle of attack below stall were added, the variations in dynamic pressure with azimuth would then modify the measured centers of pressure in such a way as to result in reduced one-per-revolution aerodynamic control forces. In other words, the added source of moment variation with azimuth would be expected to have a phase angle such as to offset partially the measured variations.

Discussion of Actual and Two-Dimensional-Airfoil Pressure-Distribution Differences

The reasons for the differences found between actual and two-dimensional airfoil data are not completely understood. As is well known, the flow conditions on a rotor are highly complex and many potential contributing explanations have long been at hand should such problems arise. Since the problem has now been verified in tangible form, an effort is being made to sort out some of these possibilities.

As one example, the fact that a high rate of increase in angle of attack can give higher than static $C_{N_{max}}$ values is well known (for example, ref. 3), and this effect has long been looked for in rotor measurements. In some early investigations this effect was apparently negligible, that is, stall was evidenced roughly where expected. Apparently the other complexities of rotor inflow, and the specific design details, prevented any significant occurrence of higher than static $C_{N_{max}}$ values. In several more recent investigations, including the present one, the opposite has been true. Dynamically, this effect would be expected to increase the actual amplitude of the oscillating air loads as compared to the calculated loads based on two-dimensional data.

It should be noted that the most drastic source for high rates of change of angle of attack is likely to be the striking of the tip vortex from the previous blade. Consequently, the high rates of change and the C_N values in excess of static two-dimensional values may occur in specific cases in basically mild flight conditions as well as in the low rotor speed or high forward velocity conditions normally associated with blade-section stalling.

Time-varying blade yaw angles, spanwise flow on the blade, and nonuniform velocity gradients in front of the airfoil are other possible factors that may cause disagreement between actual and two-dimensional airfoil characteristics.

CONCLUDING REMARKS

It has been shown that the actual helicopter rotor blade does not always behave in accordance with two-dimensional airfoil data. These airfoil-characteristic differences are expected to amplify both the flapwise and torsional blade oscillating loads. Possible reasons for these differences were briefly explored. The point is made that when the loads are predicted from refined inflow theories as compared with experimental loadings, caution should be exercised in interpreting differences in blade loading, since these may arise because of the lack of applicability of two-dimensional data rather than inadequacies in the inflow theory. Thus, before comparisons of actual and predicted air loads are used to determine validity of angle-of-attack calculations, each experimental case used must be reviewed for evidence of the presence or abs nce of discrepancies between the actual section aerodynamic characteristics as reflected by chordwise pressure distribution, and the section characteristics being assumed in the analysis.

REFERENCES

1. Lizak, Alfred A.: Two-Dimensional Wind Tunnel Tests of an H-34 Main Rotor Airfoil Section. TREC Tech. Rep. 60-53 (SER-58304), U.S. Army Transportation Res. Command (Ft. Eustis, Va.), Sept. 1960.

2. Scheiman, James, and Ludi, LeRoy H.: Qualitative Evaluation of Effect of Helicopter Rotor-Blade Tip Vortex on Blade Airloads. NASA TN D-1637, 1963.

3. Silverstein, Abe, and Joyner, Upshur T.: Experimental Verification of the Theory of Oscillating Airfoils. NACA Rep. 673, 1939.

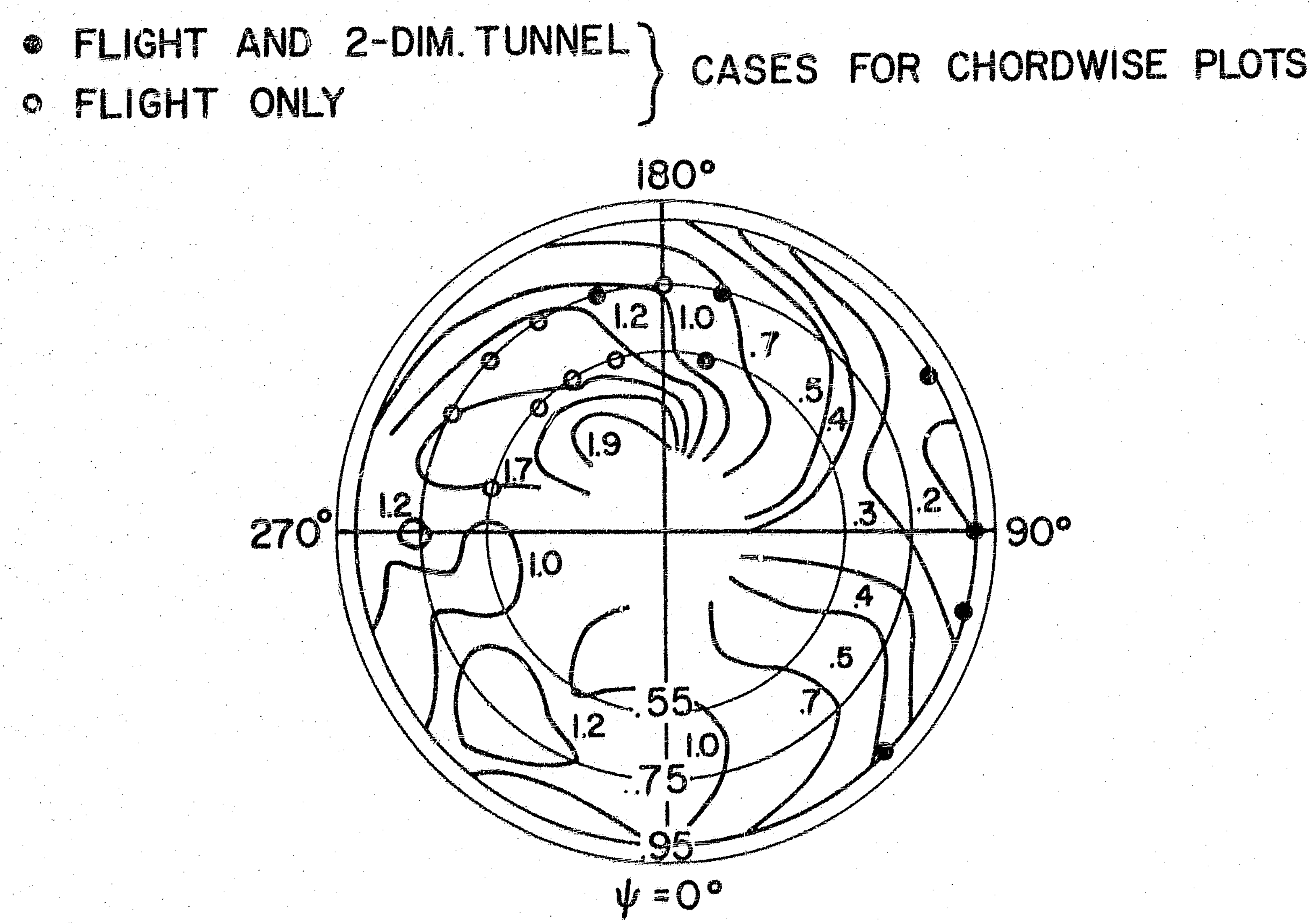

NASA

Figure 1.- Local normal-force coefficients from flight data, $\mu = 0.23$.

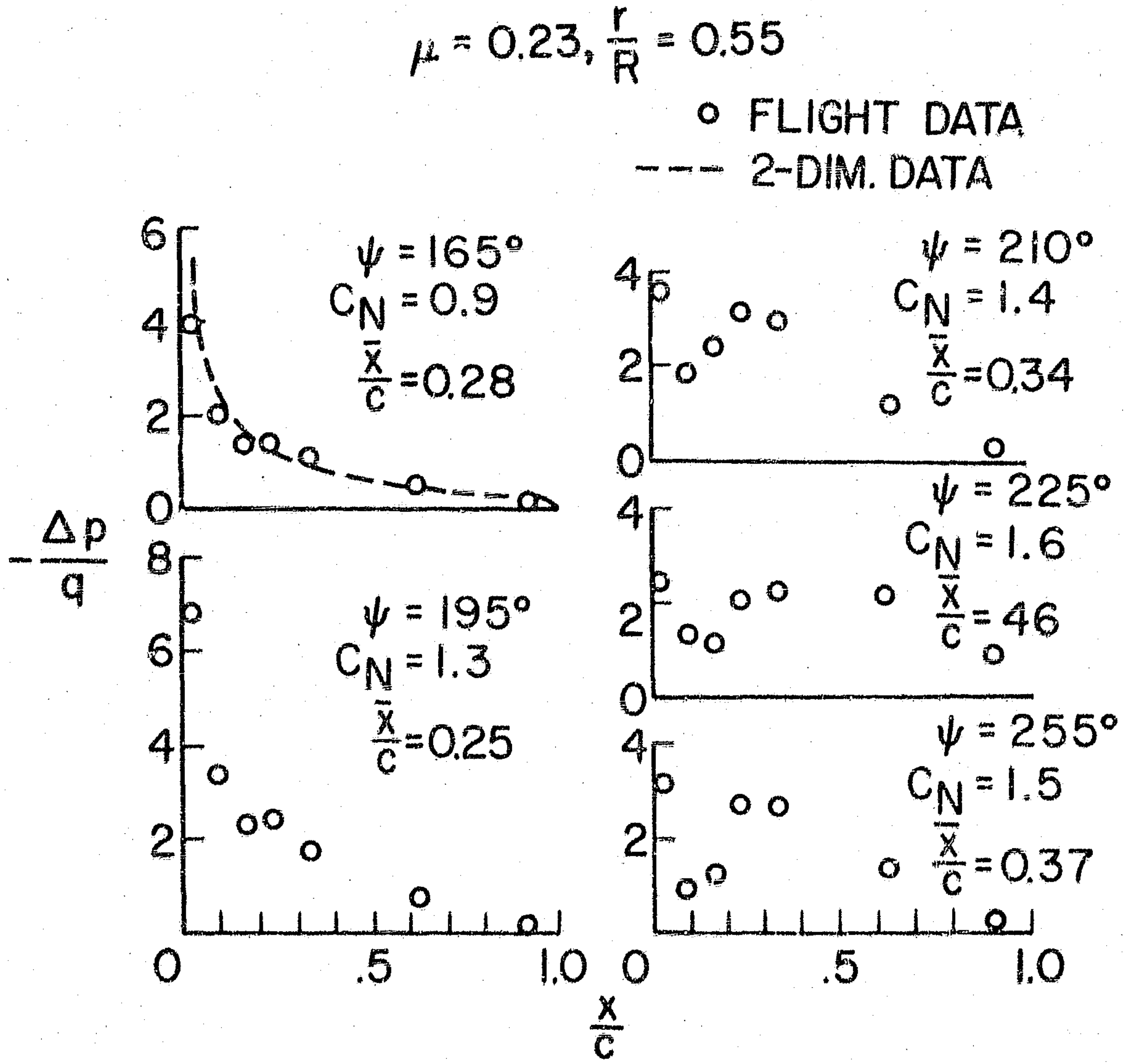

NASA

Figure 2.- Chordwise pressure distributions.

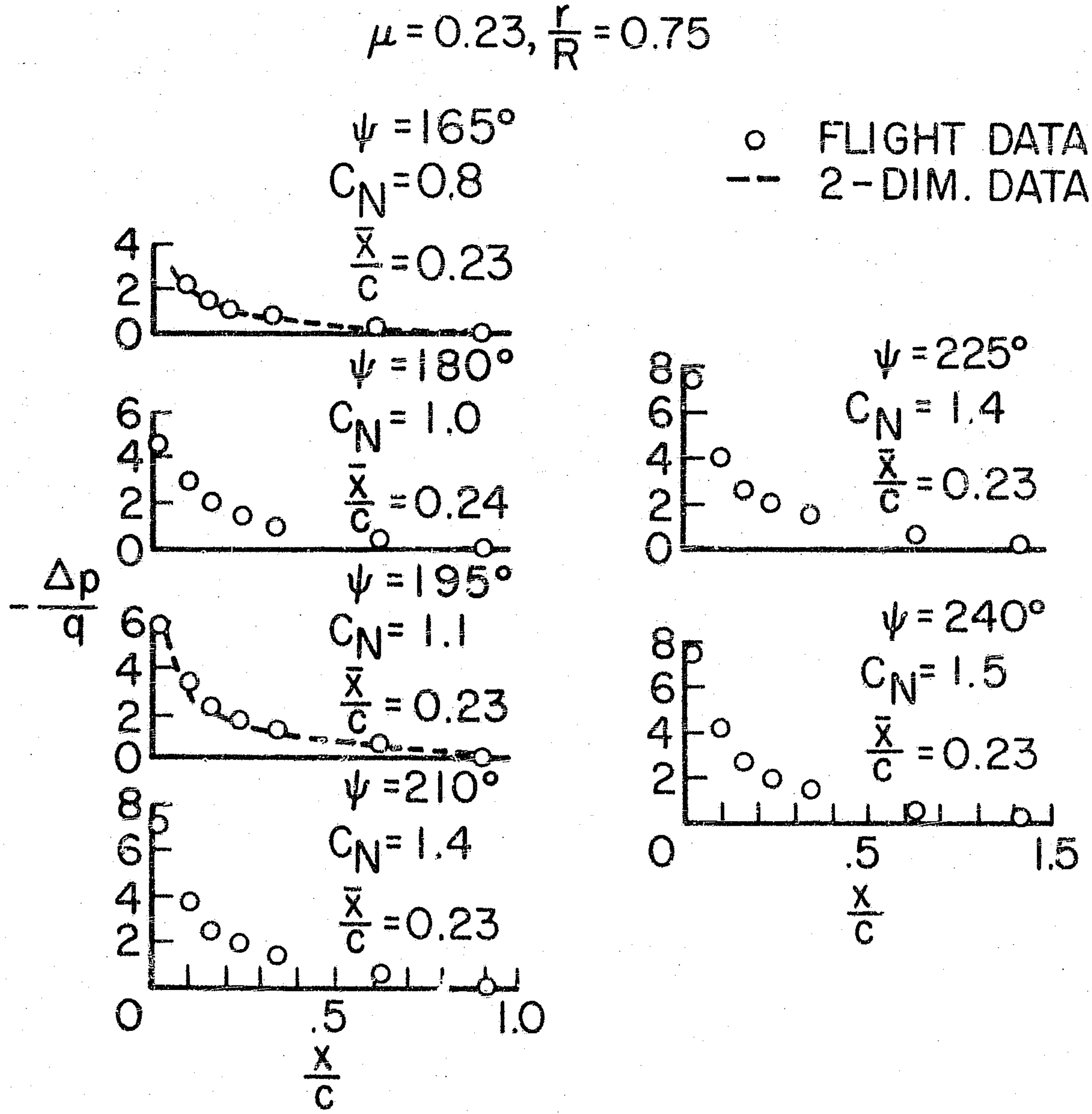

NASA

Figure 3.- Chordwise pressure distributions.

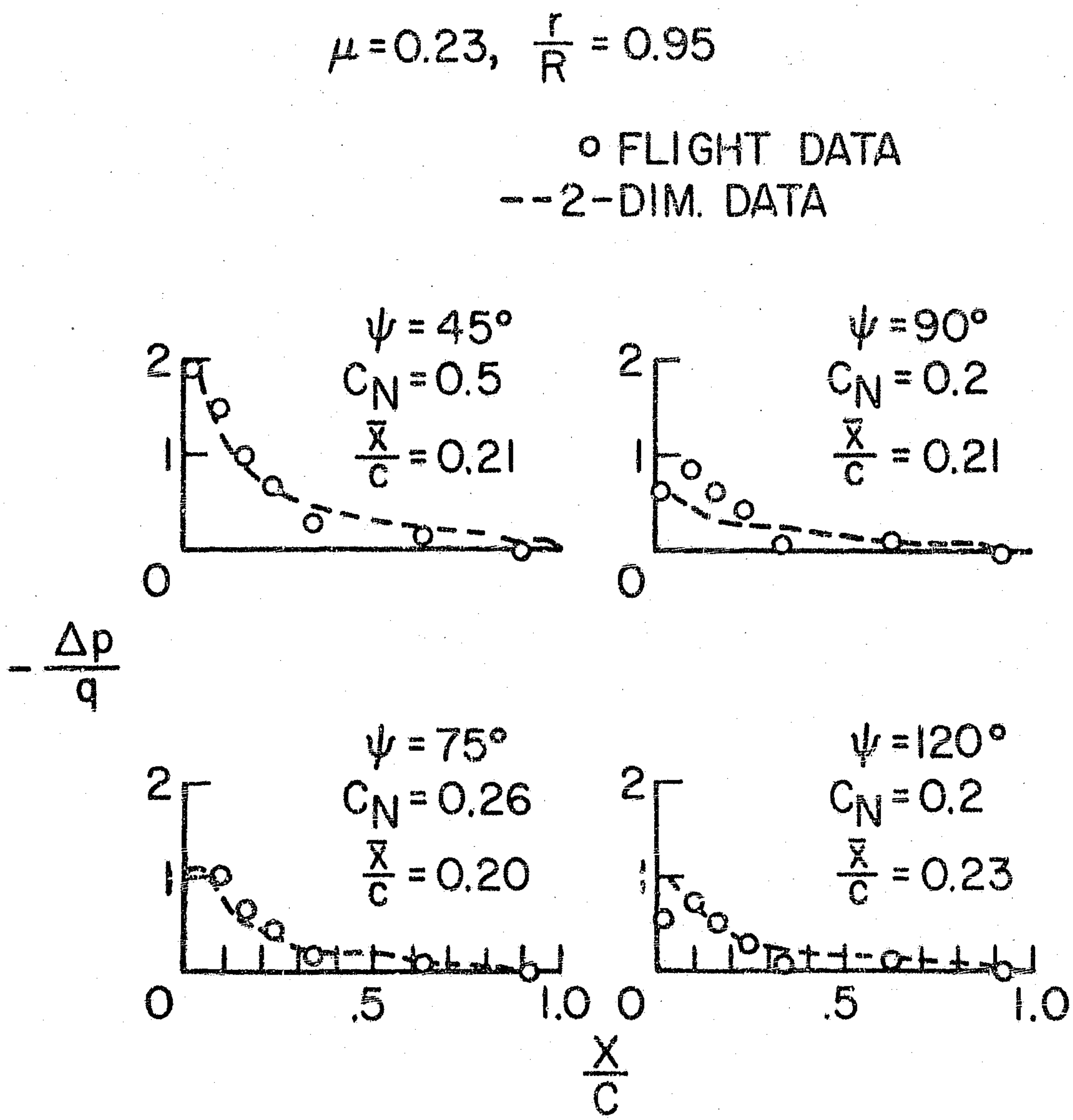

NASA

Figure 4.- Chordwise pressure distributions.

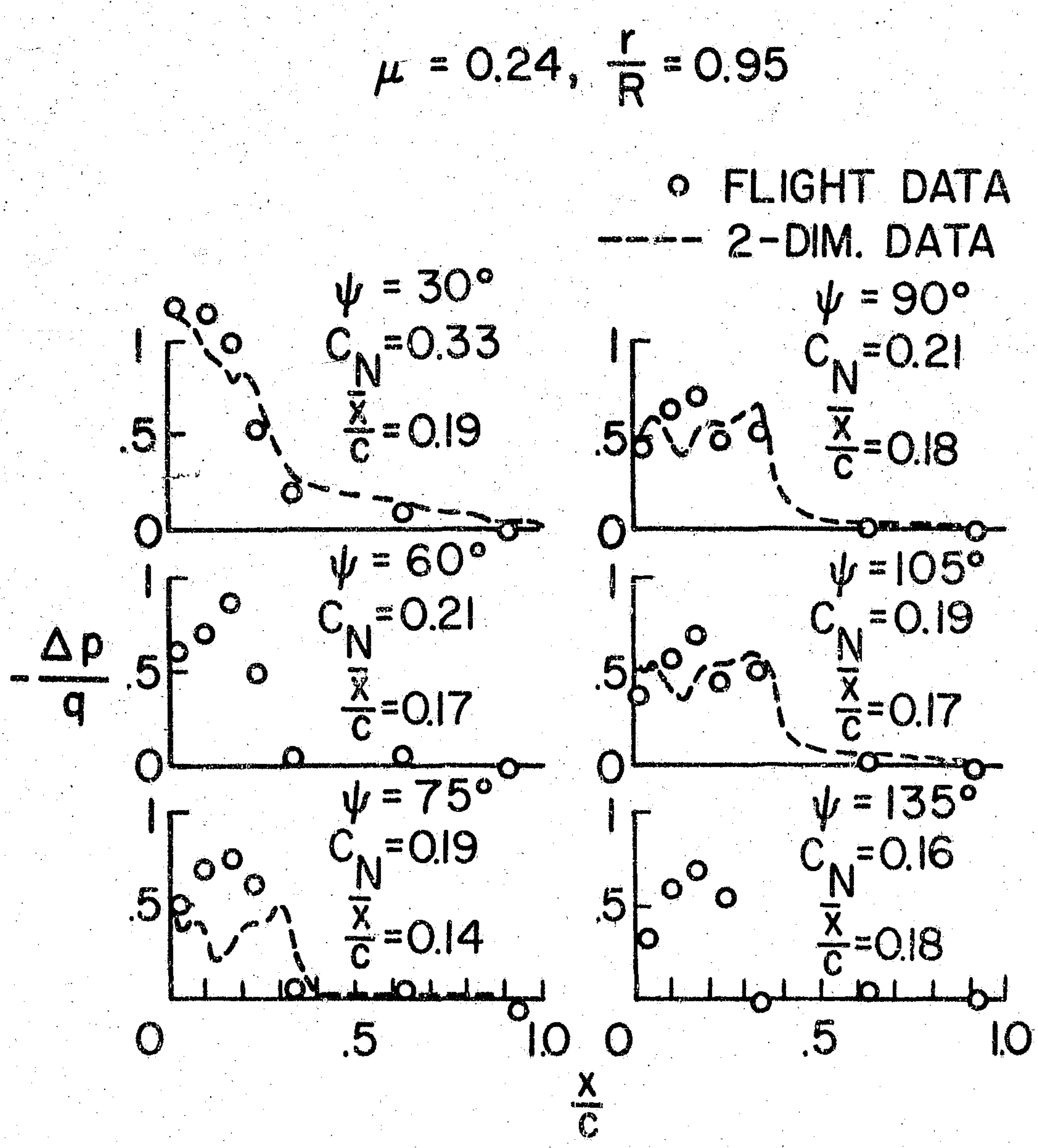

NASA

Figure 5.- Chordwise pressure distributions.

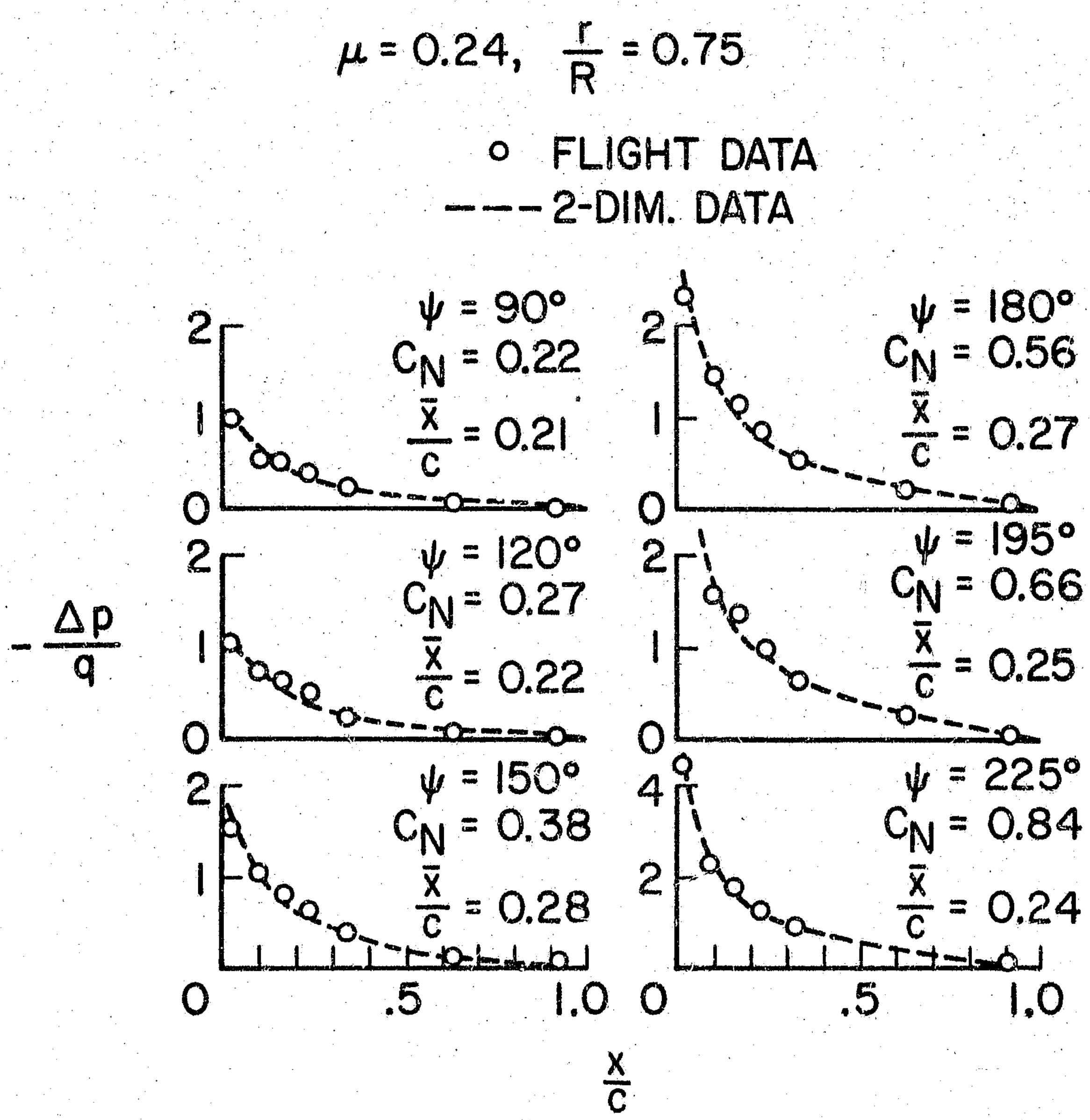

NASA

Figure 6.- Chordwise pressure distributions.

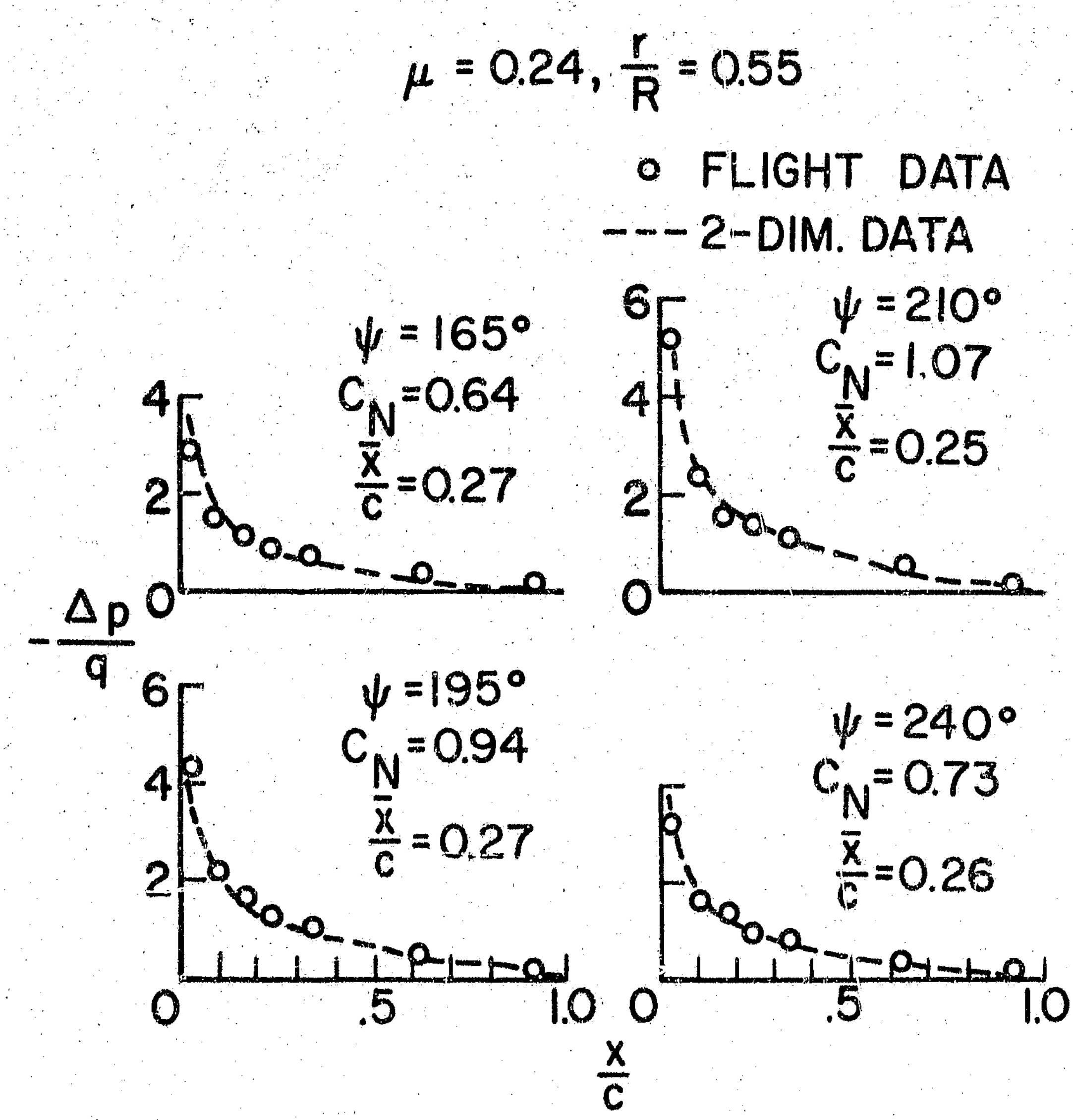

NASA

Figure 7.- Chordwise pressure distributions.

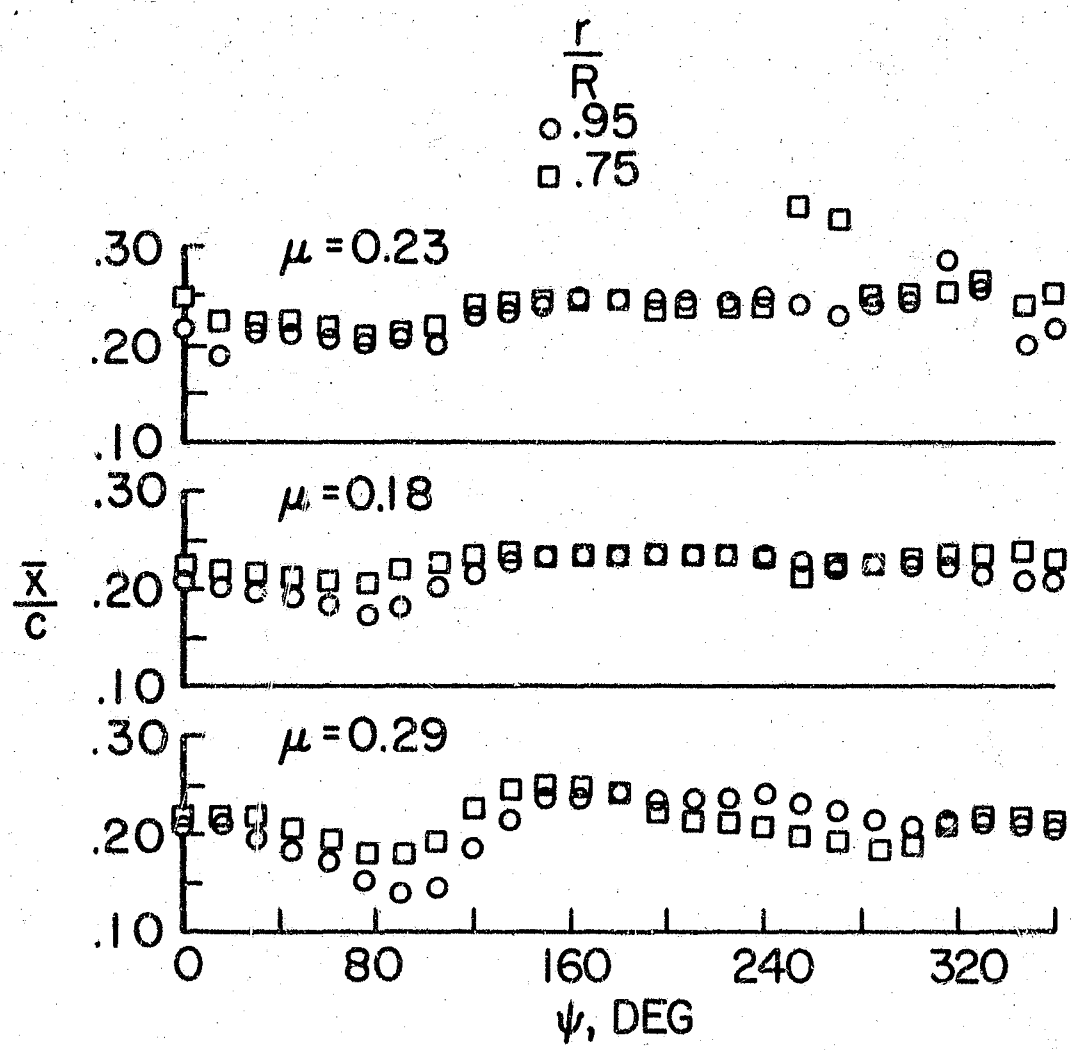

NASA

Figure 8.- Centers of pressure.